Colicin E1 Fragments Potentiate Antibiotics by Plugging TolC

S. Jimmy Budiardjo[a], Jacqueline J. Deay[b], Anna L. Calkins[c], Virangika K. Wimalasena[b], Daniel Montezano [b], Julie S. Biteen[c] and Joanna S.G. Slusky[a,b,1]

[a]Center for Computational Biology, The University of Kansas, 2030 Becker Dr., Lawrence, KS 66045-7534 [b]Department of Molecular Biosciences, The University of Kansas, 1200 Sunnyside Ave. Lawrence KS 66045 [c]Department of Chemistry, University of Michigan, Ann Arbor MI 48109-1055

[1]To whom correspondence may be addressed. E-mail: slusky@ku.edu 785-864-6519

Abstract

The double membrane architecture of Gram-negative bacteria forms a barrier that is effectively impermeable to extracellular threats. Accordingly, researchers have shown increasing interest in developing antibiotics that target the accessible, surface-exposed proteins embedded in the outer membrane. TolC forms the outer membrane channel of an antibiotic efflux pump in *Escherichia coli*. Drawing from prior observations that colicin E1, a toxin produced by and lethal to *E. coli*, can bind to the TolC channel, we investigate the capacity of colicin E1 fragments to 'plug' TolC and inhibit its efflux function. First, using single-molecule fluorescence, we show that colicin E1 fragments that do not include the cytotoxic domain localize at the cell surface. Next, using real-time efflux measurements and minimum inhibitory concentration assays, we show that exposure of wild-type *E. coli* to fragments of colicin E1 indeed disrupts TolC efflux and heightens bacterial susceptibility to four common classes of antibiotics. This work demonstrates that extracellular plugging of outer membrane transporters can serve as a novel method to increase antibiotic susceptibility. In addition to the utility of these protein fragments as starting points for the development of novel antibiotic potentiators, the variety of outer membrane protein colicin binding partners provides an array of options that would allow our method to be used to inhibit other outer membrane protein functions.

Significance

We find that fragments of a protein natively involved in intraspecies bacterial warfare can be exploited to plug the *E. coli* outer membrane antibiotic efflux machinery. This plugging disables a primary form of antibiotic resistance. Given the diversity of bacterial species of similar bacterial warfare protein targets, we anticipate that this

method of plugging is generalizable to disabling the antibiotic efflux of other proteobacteria. Moreover, given the diversity of the targets of bacterial warfare proteins, this method could be used for disabling the function of a wide variety of other bacterial outer membrane proteins.

Introduction

In Gram-negative bacteria, the concentric structures of the outer membrane, cell wall, and cytoplasmic membrane protect the cell from extracellular threats. Of these protective structures, the outer membrane is a particularly formidable barrier (1), owing to the impermeable structure of the lipopolysaccharide (LPS) that constitutes the outer membrane's outer leaflet (2). The primary means by which external molecules can gain access to the cell is through the ~100 varieties of barrel-shaped proteins that are embedded in each bacterium's outer membrane (outer membrane proteins, OMPs) (3), and whose diverse functions include the transport of molecules across the membrane—specifically, the import of nutrients and metabolites and the export of toxins and waste.

Because they are accessible from outside the cell, OMPs are attractive targets for the development of novel antibiotics, and research in this vein has begun to reveal the therapeutic potential of interfering with OMP structure and function. One recent study in *Escherichia coli*, for example, showed that exposing bacteria to a monoclonal antibody that inhibits OMP folding produces bactericidal effects (4). An alternative approach for targeting OMPs is the development of molecular plugs that block the pores of these proteins: such a plug would allow for the manipulation of bacterial transport, providing a means of either starving the bacterium (by preventing the influx of valuable nutrients) or poisoning it (by preventing the outflow of toxins). This idea of blocking the channel of outer membrane efflux pumps has been previously proposed for increasing bacterial

susceptibility to antibiotics (5). However, no successful examples to date have been reported.

In this study, we find that fragments of colicin E1—a bactericidal toxin produced by and lethal to *E. coli*—can block the capacity of TolC, an OMP in *E. coli*, to eliminate antibiotics.

TolC is the outer membrane component of the acridine efflux pump (along with AcrA in the periplasm and AcrB in the inner membrane) (6), which extrudes multiple classes of antibiotics such as erythromycin, chloramphenicol, tetracycline, doxorubicin, and acriflavine (7, 8), as well as other compounds such as bile salts and detergents (9). Deletion of TolC has been shown to render *E. coli* vulnerable to a wide variety of antibiotics (10). Moreover, expression of TolC is linearly correlated to antibiotic resistance in clinical isolates of *E. coli* (11). These observations suggest that identifying means of targeting TolC might provide insights that can contribute towards disabling antibiotic resistance, which is becoming a world-wide threat (12, 13).

Colicins are *E. coli*-specific bacteriocins, which are protein toxin systems through which bacteria engage in ‘bacterial warfare’ with other, similar bacteria. Bacteriocins hijack the OMPs of a target bacterium to cross its impermeable outer membrane and kill the bacterium. *E. coli* produces numerous types of colicins, which vary in their receptor targets and killing mechanisms. Yet, all colicins share a common triadic domain architecture, comprising the following components: (i) an N-terminal translocation (T) domain, (ii) a receptor-binding (R) domain, and (iii) a C-terminal cytotoxic (C) domain (Fig. 1*A*). Colicin import is initialized by the binding of the R domain to an OMP target with high affinity (14, 15); this binding localizes the colicin onto the outer membrane. Once colicin is tethered to the outer membrane surface, the T domain initiates translocation using a secondary OMP receptor that is, in most cases, distinct from the R

92 domain's OMP target (16). Colicin E1 uses TolC as the receptor of the T domain and
93 BtuB as the receptor of the R domain (17).
94 Prior studies have suggested that segments of colicin E1's T domain can bind the
95 TolC channel (18). In particular, peptides including residues 100-120 of colicin E1
96 (termed the 'TolC box'), with additional amino acids at the C-terminus of the 'box', have
97 been shown to co-elute with TolC (18) and to disrupt channel conductance (19). A
98 subsequent study confirmed the identity of the minimal T-domain segment that binds
99 TolC, showing that *E. coli* exposure to peptides comprising residues 100–120 is
100 sufficient to prevent subsequent binding of full-length colicin E1 (as reflected in the fact
101 that the bacteria were protected from the colicin's cytotoxic effects (20)). Notably, none
102 of these studies investigated the effects of exposure to colicin E1 fragments on TolC's
103 efflux activity.
104 Accordingly, here we use specific fragments of colicin E1 to determine whether the
105 binding event between the N-terminal T domain and the TolC pore can disrupt the
106 OMP's native export function. In particular, we suggest that this binding event is likely to
107 plug the pore, in light of observations, obtained through circular dichroism, that colicin E1
108 inserts into the TolC *β*-barrel as a helical hairpin (18). The proposed plugging
109 mechanism is further supported by co-crystal structures of colicin E3 and E9 fragments
110 bound to the outer membrane porin OmpF, which revealed that the peptides obstruct the
111 OmpF barrel (21, 22).
112 We investigate minimal truncations of colicin E1 that include the entirety of the T and
113 R domains (colE1-TR), the T domain alone (colE1-T), and a peptide containing residues
114 100-143 (colE1-$T_{100\text{-}143}$), i.e., the TolC box together with 23 additional residues (Fig. 1*B*).
115 Inclusion of the additional residues in the latter peptide was motivated by the observation
116 that colE1-T forms a helical hairpin and that colicin E1 is theorized to also insert into
117 TolC as a helical hairpin (23), and a transmembrane hairpin requires ~43 amino acids.

Through real-time efflux assays, minimum inhibitory concentration (MIC) experiments, and single-molecule microscopy, we find that colE1-TR and colE1-T are able to inhibit TolC-mediated efflux. Importantly, we find that extracellular plugging of TolC reduces the amount of antibiotics required to inhibit the growth of these bacteria—indicating that this colicin E1 fragment reduces the antibiotic resistance conferred by TolC. This work points to the potential for using colicin fragments for bacterial species-specific antibiotic potentiation and, more broadly, for species-specific blocking of the import/export functions of OMPs.

Results

Colicin E1 Localization. To determine the utility of our colicin E1 truncations as plugs for antibiotic efflux, we used an extracellular protease digestion assay to assess whether colE1-T and colE1-TR localize on the cell surface or translocate across the outer membrane. Stalling on the outer membrane surface would

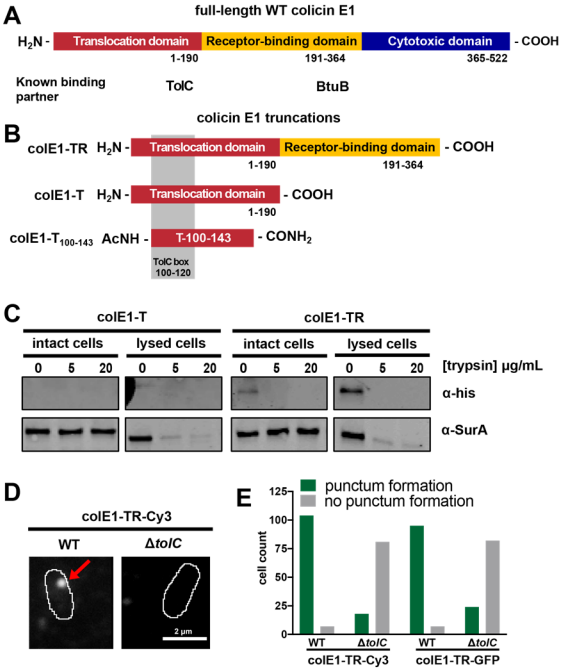

Fig. 1: Colicin E1 domains and cellular localization. Domain architecture of colicin E1. (A) Full-length colicin E1, showing sections known to bind to OMP targets. The T domain (blue) interacts with TolC; the R domain (yellow) interacts with BtuB; and the C domain is delivered to the inner membrane. (B) Truncation constructs used in this study to evaluate TolC plugging. colE1-TR lacks the C-terminal cytotoxic domain; colE1-T lacks both the cytotoxic and R domains; and colE1-$T_{100-143}$ includes the TolC box, a stretch of amino acids (residues 100-120) required for binding to TolC (grey box). (C) Extracellular protease digest assay. SurA used as a periplasmic localization and membrane integrity control (D) Fluorescence image of Cy3-labeled colE1-TR overlaid on outlines of living *E. coli* cells from phase-contrast microscopy for WT and Δ*tolC*. Red arrow indicates a punctum of 12-20 colE1-TR molecules on the cell surface. Scale bar: 2 µm. (E) Counts of cells where colE1-TR-Cy3 punctum formation was observed for WT and Δ*tolC*.

render the proteins susceptible to digestion when trypsin is in the extracellular environment. Conversely, if the protein translocates into the intracellular environment, the outer membrane should shield the protein from digestion.

Colicin localization was probed through western blot analysis of specific colicin fragments with C-terminal polyhistidine-tags. Cells were incubated with these colicin fragments and subsequently exposed to two increasing concentrations of trypsin. If the protein enters the cell, the outer membrane shields it from trypsin digestion and a corresponding band is present on the western blot under conditions with trypsin (intact cell condition). Periplasmic protein SurA was used as a membrane integrity control to identify if trypsin entered cells. As a trypsin activity control, half of the cell sample was lysed (lysed cell condition) exposing all cellular compartments to trypsin.

When we probed colE1-T for interaction with the cell, there was no detectable level of the protein either in the presence or in the absence of trypsin (Fig. 1*C*, left), indicating lack of binding. When cells were incubated with colE1-TR, a band corresponding to colE1-TR appeared on intact cells that were not exposed to trypsin. When we increased the amount of trypsin, colE1-TR was digested at each trypsin concentration, indicating that the colicin E1 fragment was localized to the outer membrane surface (Fig. 1*C*, right). In contrast, the control, periplasmic chaperone SurA, was not degraded at any trypsin concentration unless the cells were lysed before the digestion reaction (24).

After determining that colE1-TR remains at the cell surface, we probed binding and cell localization through single-molecule fluorescence microscopy. C-terminal cysteines were incorporated into colE1-T and colE1-TR to enable thiol coupling to the fluorescent dye cyanine 3 (Cy3). When colE1-TR-Cy3 was added to the extracellular environment of WT BW25113 *E. coli* cells (containing TolC), distinct puncta (Fig. 1*D*, left) formed on 94% of the cells (n = 111) (Fig. 1*E*). In strain JW5503-1, a population of

cells lacking TolC (Δ*tolC*), puncta were observed in only 18% of cells (*n* = 99) (Fig. 1*D*, right, Fig. 1*E*). In WT and Δ*tolC* cells that did feature puncta, colE1-TR formed clusters of 12–20 molecules per punctum, where each cluster had a diameter of less than the microscope's 0.5 μm resolution. The quantity of molecules and the size of the puncta were in agreement with previous studies of BtuB clusters (25, 26), supporting the assumption that the puncta comprised clusters of colE1-TR bound to BtuB. We further verified that punctum formation and localization was not an artifact of Cy3 conjugation: a fusion construct of GFP to the C-terminus of colE1-TR also displayed the same cluster formation characteristics (Fig. 1*E*, *SI Appendix,* Fig. S1*A*). No other single protein binding events were detected aside from the observed puncta formation in either WT or Δ*tolC* cells. A Δ*btuB* strain is not commercially available. Both strains of the Keio collection marked Δ*btuB* were found to have reverted by the Coli Genetic Stock Center (personal communication). Although there have been truncations described in the literature, we anticipate that at least some of the protein is required for survival.

Colicin constructs lacking the R domain (colE1-T-Cy3) showed no detectable binding either to WT cells containing TolC or to the TolC knockout strain of cells (*SI Appendix*, Fig. S1*B*), indicating that the TolC:colE1-T interaction is much weaker than the BtuB:colE1-TR interaction. Moreover, when we observed time courses of bound colE1-TR, all puncta remained immobile for > 5 minutes (Movie S1), further supporting the proposition that colE1-TR does not translocate (27) and that it binds to BtuB. Limited mobility of BtuB in the membrane has previously been observed; specifically, fluorescently-labeled BtuB did not show fluorescence recovery after photobleaching (FRAP) on long time scales (28).

Taken together, our observations are consistent with a model in which colicin E1 initially binds to BtuB, and in which TolC subsequently improves the interaction, and thus increases the frequency of cluster formation. Because the T-domain did not show any

195 binding in either localization experiment, we did not test the TolC box containing peptide
196 colE1-$T_{100-143}$.
197
198 **Colicin E1 Binding to TolC.** Since binding of colE1-T to TolC was not detectable in our
199 cell-based experiments, we wanted to ensure that our colicin E1 constructs indeed bind
200 to TolC in vitro. The interaction of TolC and colicin E1 fragments has previously been
201 characterized in vitro through co-elution of the peptides by size exclusion chromatograph
202 (SEC) (18). We used a similar approach and assessed peak shifts for both colE1-T and
203 colE1-TR when mixed with TolC. ColE1-T alone and TolC alone eluted from the SEC at
204 14.7 mL and 10.7 mL, respectively (Fig. 2A, right). When the two were mixed together,
205 we observed shift in the TolC peak to 10.2 mL and a decrease in intensity associated
206 with the colE1-T peak indicating that a subset of the population has migrated with TolC.
207 We analyzed the peak (arrow) using sodium dodecyl sulfate polyacrylamide gel
208 electrophoresis (SDS-PAGE) (Fig. 2A, left) and found the presence of both colE1-T (red
209 triangle) and TolC (purple triangle), indicating the colE1-T co-elutes with TolC. ColE1-TR

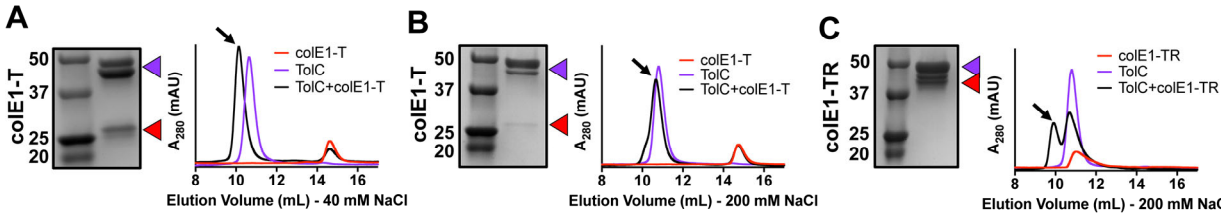

Fig. 2: Colicin E1 fragments bind to TolC *in vitro*. Co-elution experiment to determine binding of colE1-T (red line) and colE1-TR (red line) to TolC (purple line). The arrow indicates the co-elution (black line) fractions that were analyzed by SDS-PAGE. TolC runs as a double band at ~50kDa as a monomer. Red arrows indicate the presence of colicin E1 constructs that have co-eluted with TolC (purple arrows). (A) Co-elution of colE1-T with TolC at 40mM NaCl (B) Co-elution of colE1-T with TolC at 200mM NaCl (C) Co-elution of colE1-TR with TolC at 200mM NaCl. The T domain did not show binding in our *in vivo* experiments but binds to TolC *in vitro*. colicinE1-TR precipitates in 40mM NaCl so it could not be evaluated for binding with TolC under these conditions.

210 precipitates in the NaCl concentration (40 mM) used to co-elute colE1-T so we increased

the salt concentration to 200 mM. Under the higher salt concentration, when TolC and colE1-T are mixed there is a smaller peak shift and the presence of a shoulder (Fig. 2B, right). Although we could detect binding, the higher salt concentration prevents full binding as indicated by a much fainter band for colE1-T (Fig. 2B, left).

When TolC and colE1-TR were mixed (Fig. 2*C*, right), we observed a peak shift from 11.0 mL for colE1-TR alone to 10.0 mL for colE1-TR in the presence of TolC. The more drastic shift (as compared with the shift observed for colE1-T) can be attributed to the additional mass associated with the R domain. Again, analysis with SDS-PAGE (Fig. 2*C*, left) revealed that both colE1-TR (red) and TolC (purple triangle) bands were present.

Colicin E1 Inhibits Active Efflux. Real-time efflux inhibition by colicin E1 fragments was assessed using a live-cell assay with N-(2-naphthyl)-1-naphthylamine (NNN)-dye, which is effluxed by the acridine efflux pump and fluoresces when it is localized inside the cell (29). Efflux of NNN can be turned off by the protonophore CCCP, which neutralizes the proton motive force allowing for accumulation of the dye within the cell. Active efflux can then be monitored by the decay in fluorescent signal once proton motive force is reenergized by the addition of glucose (29-33).

We assessed the ability of colicin E1 truncations to plug TolC by monitoring real-time efflux of NNN. Cells exposed to colE1-$T_{100\text{-}143}$ (comprising colicin E1 residues 100-143; Fig. 1*B*) did not show lower real-time efflux of the fluorescent probe molecule NNN (i.e., weaker decay in fluorescence), as compared with untreated cells **(**Fig. 3*A*). This observation is notable in light of the fact that, in previous studies, similar peptides were shown to bind TolC (18, 20) and to occlude the channel, as reflected in diminished

conductance (18, 19). These studies, however, did not investigate the effects of colicin E1 fragments on the efflux function of the pump.

Cells exposed to colE1-T, comprising the full T domain, did show a distinctly lower decay in final fluorescence compared with untreated cells, though the treated cells did not retain their baseline fluorescence. These results indicate that colE1-T partially inhibited efflux (Fig. 3*B*). Finally, exposure to colE1-TR produced full inhibition of the acridine efflux pump, as fluorescence did not decrease after the addition of glucose (Fig. 3*C*).

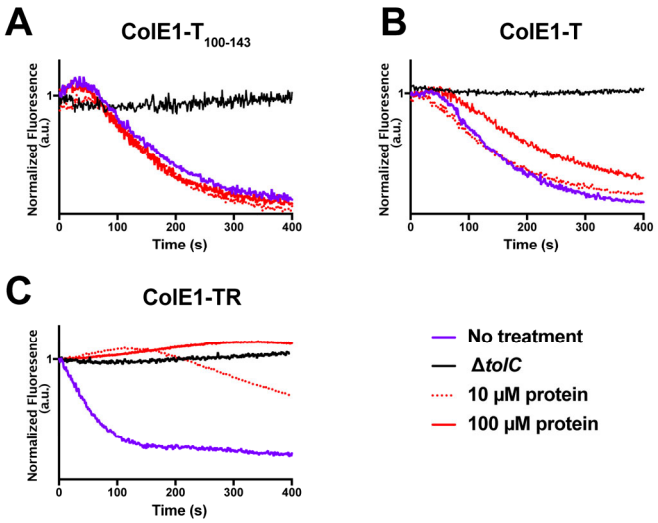

Fig. 3: Colicin E1 fragments inhibit active efflux. Effect of colicin E1 fragments on real-time efflux of N-(2-naphthyl)-1- naphthylamine (NNN) in *E. coli* WT and Δ*tolC*: (A) An N-terminal peptide fragment composed of residues 100-143 encompassing the "TolC box" (B) The entirety of colE1-T domain (C) The entirety of the T and R domains. In each case, fluorescence in WT *E. coli* with no protein is represented by a green line; Δ*tolC* is represented by a black line; WT + 10 μM protein is represented by purple dots; WT + 100 μM protein is represented by purple lines. The TolC box peptide does not show activity against NNN efflux. ColE1-T moderately inhibits NNN efflux at 100 μM. ColE1-TR shows partial inhibition at 10 μM and full inhibition at 100 μM.

Colicin E1 Increases E. coli Susceptibility to Antibiotics. Because exposure of cells to colE1-TR completely inhibited NNN efflux, we evaluated the capacity of this colicin E1 truncation to potentiate antibiotics through MICs. An effective TolC plug will reduce the concentration required to inhibit growth as antibiotics remain trapped within the cell. We chose representative antibiotics from four different antibiotic classes that are known TolC substrates: kanamycin, ciprofloxacin, erythromycin, and the antimicrobial agent benzalkonium chloride (corresponding to the classes aminoglycosides, fluoroquinolones,

macrolides, and quaternary ammonium compounds, respectively). Specifically, WT *E. coli* cells that were exposed to 100 μM colE1-TR in combination with each of these antibiotic substances showed substantially lower MICs (Fig. 4) compared with cells exposed to the antibiotics alone: Exposure to 100 μM colE1-TR made WT E. coli ~1.5-2.0-fold more susceptible to these antibiotics (SI Appendix, Table S1).

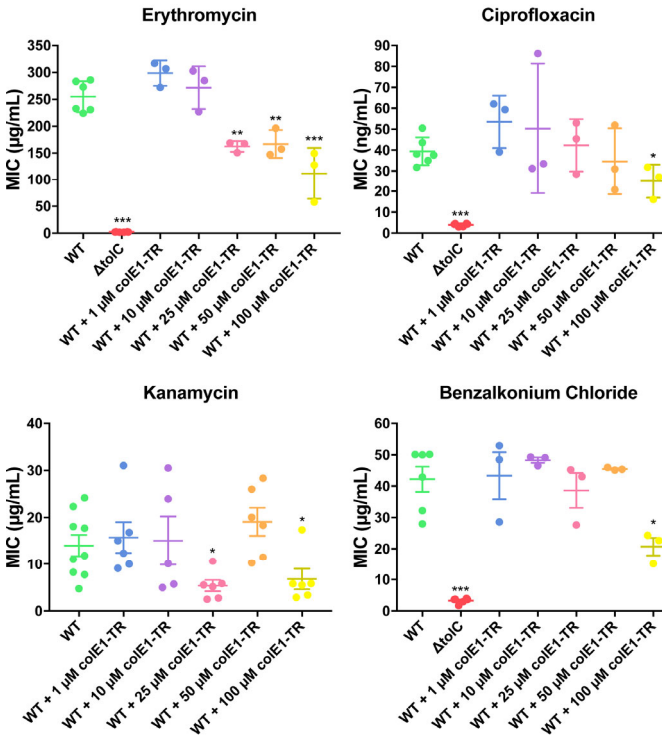

Fig. 4: ColE1-TR makes antibiotics more potent: Antibiotic susceptibility was determined in the absence (green) and presence of colE1-TR at 1 μM (blue), 10 μM (purple), 25 μM (pink), 50 μM (orange), 100 μM (yellow) for erythromycin, ciprofloxacin, kanamycin, and benzalkonium chloride in *E. coli* WT. MICs for Δ*tolC* (red) are included as a reference for total loss of TolC. For kanamycin, the MIC for Δ*tolC* was not determined since the deletion of the *tolC* gene is accomplished by insertion of a kanamycin resistance cassette. Kanamycin was collected with more replicates as the data was more variable. All data for WT were collected with biological replicates, and error bars correspond to the standard error of the mean. Clusters indicated have a statistically significant difference in their mean values relative to WT (* with $P < .050$, ** with $P < .010$, *** with $P < .001$)

Discussion

In this study, we explored a novel method of modulating OMP function in *E. coli* by plugging an outer membrane protein channel using a fragment of a protein that is produced by and lethal to these bacteria. Specifically, we leveraged the observed capacity of colicin E1's T domain to occlude TolC, and proposed that the colicin might also serve as a molecular plug that disrupts the channel's native efflux function, which facilitates the elimination of antibiotics. We found that a fragment of colicin E1 that lacks

the cytotoxic C domain potentiates antibiotics of various classes, including aminoglycosides, fluoroquinolones, macrolides, and quaternary ammonium compounds.

We first showed that colicin E1 truncations composed of the T or the TR domains, without the C domain, do not fully enter into cells. Through single-molecule microscopy we were able to observe the TR domain bind to the WT cell surface. In contrast, for colE1-T, a truncation that did not include the R domain, we did not observe binding to the cell surface. Notably, however, TolC binding did seem to have a significant role in the binding of colE1-TR to the cell surface: binding occurred in a substantially higher proportion of WT *E. coli* than in cells deleted of TolC. In Δ*tolC* cells, the few binding events that were observed were localized to puncta, and were assumed to reflect binding of the R domain to BtuB. Taken together, these observations suggest that the T domain:TolC interaction enhances colicin E1's ability to stay bound to the surface but is not sufficient on its own to show binding events. Indeed, this proposition is supported by the results of the real-time efflux functional assay, where colE1-T only partially inhibited efflux of antibiotics, whereas colE1-TR achieved full inhibition. We infer from these observations that the relative affinity of the T domain for TolC is weaker than the affinity of the R domain to BtuB. Avidity by the additional interaction of the R domain with BtuB is required for full inhibition of efflux. This is not surprising since colicin E1 functions as part of a mechanism to deliver a cytotoxic domain and not specifically for TolC plugging.

In addition to pointing to a means of manipulating TolC efflux, our observations enable us to draw conclusions regarding the mechanism of efflux inhibition. Previous functional studies have proposed two alternative models for colicin E1's utilization of TolC to enter and poison the cell (18, 34). The first is the 'total thread' model in which the entire colicin is unfolded, and TolC serves as a channel for it to thread through (34). The second, 'pillar' model, based on structural studies of the binding interaction between

TolC and N-terminal peptides of colicin E1, proposes that colicin E1 inserts into TolC as a helical hairpin, which serves as a buttress to facilitate the entry of the colicin's cytotoxic domain (18). In this model, the intrinsic properties of the cytotoxic domain itself are proposed to allow it to cross the outer membrane, potentially with mediation by anionic LPS. The results presented herein support the latter model. Specifically, we observed that, without the cytotoxic domain, colE1-TR remains stalled on the outer membrane exposed to the extracellular environment, instead of entering the cell, as would be expected with the total thread model.

Accordingly, we propose the following mechanism of efflux inhibition based on the Cramer 'pillar' model of colicin E1 interaction with BtuB and TolC. First, the R domain binds to BtuB with high affinity and acts as an anchoring point for the colicin on the cell membrane (Fig. 5*A*). Second, the T domain is able to search for TolC and insert into the channel, stabilizing its association with the membrane and, more importantly, forming a plug that blocks the exit of TolC substrates (Fig. 5*B*).

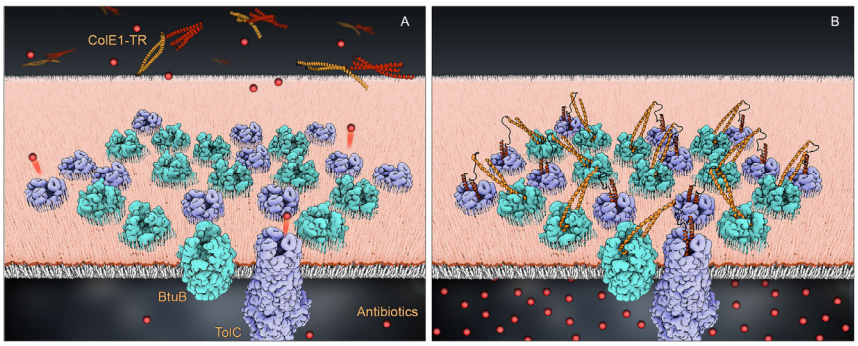

Fig. 5: Model of colE1-TR inhibition of efflux. The R domain of colE1-TR (orange) binds to BtuB (cyan) with high affinity and anchors colE1-TR to the surface of the cell. The T domain (red) then inserts into TolC (lavender), plugging the channel and blocking exit of antibiotics (*spheres*). We only see this interaction when 12 or more colE1-TR bind in the same cluster. (A) Before binding, antibiotics are effluxed (B) the pillar model is depicted as a possible binding configuration that prevents efflux.

Since the presence of TolC enhances puncta formation, both BtuB and TolC need to be in close proximity for binding to occur. Given that BtuB clusters together—potentially excluding TolC—the number of full binding sites available for the T and R domains of colicin E1 may be substantially lower than simply

the number of TolC or BtuB proteins. In principle, the resolution of our microscopy experiments can detect single binding events, yet we only observe puncta with 12 binding events or more of colE1-TR to the cell surface. We speculate that there may be geometric constraints on a cluster. It may be the case that there are not sufficient TolC and BtuB oriented in such a way that at least 12 ligands can bind to both TolC and BtuB at once. To understand the order of the geometric constraint, we can create a simple model of the problem as a six by four grid allowing for 12 TolCs and 12 BtuBs. If each of these 24 proteins can be placed in any configuration on the grid, this results in the number of possible configurations at 24 choose 12 equals 2,704,156 (*SI Appendix*, methods). The number of configurations in which all 12 TolCs would be adjacent to a BtuB is a small percentage of these configurations. Using the Hopkraft-Karp algorithm (SI Appendix, methods) we determined how many of these conformations would have all TolC paired to a BtuB by being in one of BtuB's eight adjacent squares. We find only 262,912 confirmations or 10% of the total possible arrangements-- suggesting that the availability for binding within a cluster is a low probability event.

Though it seems that colicin E1 confers a dose response of antibiotic potentiation, the relatively high concentration of colE1-TR needed to significantly inhibit efflux may be at least partially explained by these geometric considerations as well as by other binding concerns. Although previous studies have identified nanomolar affinities between BtuB and the R domain of colicin E3 (14, 35), in a competition assay where excess BtuB was shown to protect cells from colicin E3, no protection from colicin E1 was observed, even at 200 molar excess (36). The latter observation indicates that the binding affinity between colicin E1 and BtuB is lower than that between colicin E3 and BtuB, and may reflect the fact that, as observed here, TolC has a significant role in colicin E1 binding. At an OD_{600} = 1 we anticipate approximately 8 x 10^8 *E. coli* cells, each with approximately 400 BtuBs (37) and 1,500 trimeric TolCs (38). A back-of-the-

363 envelope calculation indicates that at a 100μM concentration, colE1-TR has 50,000
364 colE1-TR domains for every TolC pore in the sample. Though 10 μM colE1-TR was
365 sufficient to affect efflux of NNN, this quantity did not stop efflux completely, and was not
366 sufficient to heighten cells' sensitivity to antibiotics. Though we cannot explain why quite
367 such a high concentration is necessary for antibiotic potentiation, it is clear that for this
368 method of antibiotic potentiation to be useful the binding affinity between the T domain
369 and TolC will need to be increased.

370 Owing to their limited potency, our colE1-T and colE1-TR fragments are not likely
371 to be useful in direct practical applications of antibiotic potentiation. However, as a proof
372 of concept, our findings offer a potential roadmap for further development. A more potent
373 binder of TolC would not need the R domain anchor. If the interaction between TolC and
374 colE1-T can be resolved to atomic detail, the colicin T domain would serve as an ideal
375 candidate for optimization by computational methods and/or by directed evolution to
376 engineer an effective antibiotic potentiator to prevent the spread of antibiotic resistance.
377 Moreover, once the atomic structure of the interaction is known, proteins could be
378 designed for blocking efflux through outer membrane efflux pumps of at least five other
379 bacterial organisms. Each of these organisms have structurally characterized outer
380 membrane efflux pumps that have been shown to be homologous and structurally similar
381 to TolC (39).

382 More broadly, there are more than 20 known varieties of bacteriocins. These
383 bacteriocins are known to bind to different bacterial outer membrane proteins with a wide
384 variety of functions including: adhesion, iron transport, and general import (16, 40).
385 Applying this method of inhibition using fragments derived from other colicins may
386 provide insight into inhibition of other bacterial function as well.

387

Materials and Methods

A complete description of materials and methods is available as supporting information.

E. coli strains

E. coli strains BW25113 and JW5503-1 were purchased from the Coli Genetic Stock Center (CGSC). JW5503-1 is a tolC732(del)::kan from the parent strain BW25113. BL21(DE3) were used for expression of the colicin constructs. BL21(DE3)Omp8 (a generous gift from the D. Müller) was used to express TolC.

Expression and Purification

Colicin E1 constructs

Genes for colicin constructs (colE1-T, colE1-TR, colE1-T-E192C, colE1-TR-E366C, colE1-TR-GFP) were cloned into pET303. Plasmids were transformed into BL21(DE3) and proteins were expressed in TB media supplemented with 0.4% glycerol, 10 mM MgCl2. Protein expression was induced with 1mM IPTG at 15 °C for 24 hours. Proteins were purified by nickel affinity chromatography followed by gel filtration on an ÄKTA pure chromatography system.

TolC

Full-length TolC was cloned into pTrcHis with a C-terminal 6x histidine tag and transformed into BL21(DE3)Omp8. Protein expression was induced with 1mM IPTG at 25 °C for 24hrs. TolC was extracted from the membrane fraction with 1% n-dodecyl-β-D-maltoside at 4 °C for 24hrs and purified by nickel affinity chromatography followed by gel filtration on an ÄKTA pure chromatography system.

Peptide Synthesis

412 ColE1-$T_{100-143}$ was synthesized using a CEM liberty blue microwave peptide synthesizer
413 using standard Fmoc chemistry. The peptides where cleaved using a solution of
414 92.5:2.5:2.5:2.5 TFA:TIPS:H2O:DoDt and the crude peptides where purified using
415 preparative HPLC. Analytical HPLC traces were acquired using an Agilent 1100
416 quaternary pump and a Hamilton PRP-1 (polystyrene-divinylbenzene) reverse phase
417 analytical column (7 µm particle size, 4 mm x 25 cm) with UV detection at 215 nm. The
418 eluents were heated to 45 °C to reduce separation of rotational isomers, and elution was
419 achieved with gradients of water/ acetonitrile (90:10 to 0:100 containing 0.1% TFA) over
420 20 min. Low-resolution mass spectra (LRMS) were obtained using a Waters Micromass
421 ZQ 4000 instrument with ESI+ ionization
422
423 Extracellular Protease Digestion
424 Protein localization after exogenous addition to whole cells was determined as
425 previously described (24). Briefly, colE1 protein constructs were incubated with whole
426 cells followed by trypsin digestion. If colE1 enters the cell it would be protected from
427 trypsin digest by the cell membrane. If colE1 remains localized to the outer membrane it
428 would by susceptible to trypsin digestion. The presence of ColE1 was probed through
429 western blot analysis.
430
431 Single-Molecule Microscopy
432 Cysteine mutants were labeled with Cyanine 3 (Cy3) through maleimide chemistry.
433 BW25113 or Δ*tolC* were mixed with Cy3 labeled colicin E1 (T or TR) or colE1-TR-GFP
434 and imaged (live and unfixed) using epifluorescence microscopy with sensitivity to detect
435 single dye molecules as described previously (41). Fluorescence was excited by a 561-
436 nm laser (Coherent Sapphire 560-50) for Cy3 or a 488-nm laser (Coherent Sapphire
437 488-50) for GFP. Fluorescence was imaged with an Olympus IX71 inverted microscope

with a 100x, 1.40-NA oil-immersion objective. Images were captured with a Photometrics Evolve electron multiplying charge-coupled device (EMCCD) camera.

Co-elution

The interaction of TolC and colicin E1 T or TR were determined by co-elution on an SEC column. Purified TolC and colicin E1 T or TR were mixed at a 1:2 molar ratio and incubated at room temperature for 1 hour before loading onto a Superdex 200 Increase 10/300 GL column (GE Healthcare). The protein was eluted with 1.5 column volumes into 20 mM Tris pH 8.0, 40 mM NaCl, 0.05% n-dodecyl-β-D-maltoside for colE1-T. For colE1-TR the NaCl concentration was increased to 200 mM to prevent precipitation. Elution fractions were collected every 0.5 mL. Peak fractions were concentrated to 20 µL and analyzed by SDS-PAGE.

Real-time Efflux

Real-time efflux activity in the presence of colE1-TR was determined as previously described with some modifications (29, 30). Cells were resuspended to in cold PBS with and without 10-100 µM colicin proteins and incubated for 15 minutes on ice. 100µM carbonyl cyanide m-chlorophenyl hydrazone (CCCP) was added to turn off efflux. After an additional 15 minutes the efflux dye NNN was added to the cells to 10 µM. The cells were incubated at 25 °C with shaking at 140 r.p.m. for 2 hours. Cells were harvested at 3,500g for 5 minutes and washed once in 20 mM potassium phosphate buffer pH 7 with 1mM $MgCl_2$. Cell were loaded into a quartz cuvette (Agilent Technologies). Fluorescence was measured with an Agilent Cary Eclipse fluorescence spectrophotometer with excitation wavelength of 370 nm and emission wavelength of 415 nm. Fluorescence measurements were taken every 1 second. After 100 seconds, 50 mM glucose was

added to re-energize the cells and initiate efflux, and fluorescence data were collected for an additional 600 seconds.

MICs

MICs were determined using the broth dilution method in 96 well plate format using LB media in 100 µL well volumes. Cultures were grown at 37 °C with shaking at 250 r.p.m. and OD_{600} was read on a Biotek plate reader after 20 hours. *P* values were determined using a two-tailed Student's t-test in GraphPad Prism 7.0.

Acknowledgments

We gratefully acknowledge Pinakin Sukthankar, Rik Dhar, Dwight Deay and Heather Shinogle for helpful discussions and feedback, Mark Richter for the use of his fluorometer, Rajeev Misra for the pTrc vector containing the TolC gene, Daniel Müller for the BL21(DE3)Omp8 strain, Chamani Perera for peptide synthesis, Karen Marom for editorial guidance, and Batika Saxena (Grafika Labs) for artistic assistance. We also gratefully acknowledge support from NIH award DP2GM128201 to JSGS, the Gordon and Betty Moore Inventor Fellowship to JSGS, NIH award R21-GM128022-02 to JSB, and NIGMS award P20GM113117, P20GM103638.

References

1. Alexander C & Rietschel ET (2001) Invited review: Bacterial lipopolysaccharides and innate immunity. *Journal of Endotoxin Research* 7(3):167-202.
2. Kamio Y & Nikaido H (1976) Outer membrane of Salmonella typhimurium: accessibility of phospholipid head groups to phospholipase c and cyanogen bromide activated dextran in the external medium. *Biochemistry* 15(12):2561-2570.
3. Freeman JTC & Wimley WC (2012) TMBB-DB: a transmembrane β-barrel proteome database. *Bioinformatics* 28(19):2425-2430.
4. Storek KM*, et al.* (2018) Monoclonal antibody targeting the beta-barrel assembly machine of Escherichia coli is bactericidal. *Proceedings of the National Academy of Sciences of the United States of America* 115(14):3692-3697.

5. Gilardi A*, et al.* (2017) Biophysical characterization of E. coli TolC interaction with the known blocker hexaamminecobalt. *Biochimica et biophysica acta* 1861(11 Pt A):2702-2709.
6. Wang Z*, et al.* (2017) An allosteric transport mechanism for the AcrAB-TolC multidrug efflux pump. *eLife* 6.
7. Yamaguchi A, Nakashima R, & Sakurai K (2015) Structural basis of RND-type multidrug exporters. *Frontiers in microbiology* 6:327.
8. Ramaswamy VK, Vargiu AV, Malloci G, Dreier J, & Ruggerone P (2017) Molecular Rationale behind the Differential Substrate Specificity of Bacterial RND Multi-Drug Transporters. *Scientific reports* 7(1):8075.
9. Anes J, McCusker MP, Fanning S, & Martins M (2015) The ins and outs of RND efflux pumps in Escherichia coli. *Frontiers in microbiology* 6:587.
10. Liu A*, et al.* (2010) Antibiotic Sensitivity Profiles Determined with an Escherichia coli Gene Knockout Collection: Generating an Antibiotic Bar Code. *Antimicrobial Agents and Chemotherapy* 54(4):1393-1403.
11. Swick MC, Morgan-Linnell SK, Carlson KM, & Zechiedrich L (2011) Expression of Multidrug Efflux Pump Genes acrAB-tolC, mdfA, and norE in Escherichia coli Clinical Isolates as a Function of Fluoroquinolone and Multidrug Resistance. *Antimicrobial Agents and Chemotherapy* 55(2):921-924.
12. Roope LSJ*, et al.* (2019) The challenge of antimicrobial resistance: What economics can contribute. *Science* 364(6435).
13. Ventola CL (2015) The antibiotic resistance crisis: part 1: causes and threats. *P T* 40(4):277-283.
14. Kurisu G*, et al.* (2003) The structure of BtuB with bound colicin E3 R-domain implies a translocon. *Nat Struct Biol* 10(11):948-954.
15. Buchanan SK*, et al.* (2007) Structure of colicin I receptor bound to the R-domain of colicin Ia: implications for protein import. *EMBO J* 26(10):2594-2604.
16. Cascales E*, et al.* (2007) Colicin Biology. *Microbiology and Molecular Biology Reviews* 71(1):158-229.
17. Benedetti H*, et al.* (1991) Individual domains of colicins confer specificity in colicin uptake, in pore-properties and in immunity requirement. *Journal of molecular biology* 217(3):429-439.
18. Zakharov SD, Wang XS, & Cramer WA (2016) The Colicin E1 TolC-Binding Conformer: Pillar or Pore Function of TolC in Colicin Import? *Biochemistry* 55(36):5084-5094.
19. Zakharov SD*, et al.* (2004) Colicin occlusion of OmpF and TolC channels: outer membrane translocons for colicin import. *Biophysical journal* 87(6):3901-3911.
20. Jakes KS (2017) The Colicin E1 TolC Box: Identification of a Domain Required for Colicin E1 Cytotoxicity and TolC Binding. *Journal of bacteriology* 199(1).
21. Housden NG*, et al.* (2010) Directed epitope delivery across the Escherichia coli outer membrane through the porin OmpF. *Proceedings of the National Academy of Sciences of the United States of America* 107(50):21412-21417.
22. Yamashita E, Zhalnina MV, Zakharov SD, Sharma O, & Cramer WA (2008) Crystal structures of the OmpF porin: function in a colicin translocon. *EMBO J* 27(15):2171-2180.
23. Zakharov SD, Wang XS, & Cramer WA (2016) The Colicin E1 TolC-Binding Conformer: Pillar or Pore Function of TolC in Colicin Import? *Biochemistry* 55(36):5084-5094.
24. Besingi RN & Clark PL (2015) Extracellular protease digestion to evaluate membrane protein cell surface localization. *Nature protocols* 10(12):2074-2080.

25. Rassam P*, et al.* (2015) Supramolecular assemblies underpin turnover of outer membrane proteins in bacteria. *Nature* 523(7560):333-336.
26. Chavent M*, et al.* (2018) How nanoscale protein interactions determine the mesoscale dynamic organisation of bacterial outer membrane proteins. *Nat Commun* 9(1):2846.
27. White P*, et al.* (2017) Exploitation of an iron transporter for bacterial protein antibiotic import. *Proceedings of the National Academy of Sciences of the United States of America* 114(45):12051-12056.
28. Kleanthous C, Rassam P, & Baumann CG (2015) Protein-protein interactions and the spatiotemporal dynamics of bacterial outer membrane proteins. *Curr Opin Struct Biol* 35:109-115.
29. Bohnert JA, Schuster S, Szymaniak-Vits M, & Kern WV (2011) Determination of real-time efflux phenotypes in Escherichia coli AcrB binding pocket phenylalanine mutants using a 1,2'-dinaphthylamine efflux assay. *PloS one* 6(6):e21196.
30. Bohnert JA, Karamian B, & Nikaido H (2010) Optimized Nile Red efflux assay of AcrAB-TolC multidrug efflux system shows competition between substrates. *Antimicrob Agents Chemother* 54(9):3770-3775.
31. Seeger MA*, et al.* (2008) Engineered disulfide bonds support the functional rotation mechanism of multidrug efflux pump AcrB. *Nat Struct Mol Biol* 15(2):199-205.
32. Iyer R, Ferrari A, Rijnbrand R, & Erwin AL (2015) A fluorescent microplate assay quantifies bacterial efflux and demonstrates two distinct compound binding sites in AcrB. *Antimicrob Agents Chemother* 59(4):2388-2397.
33. Misra R, Morrison KD, Cho HJ, & Khuu T (2015) Importance of Real-Time Assays To Distinguish Multidrug Efflux Pump-Inhibiting and Outer Membrane-Destabilizing Activities in Escherichia coli. *Journal of bacteriology* 197(15):2479-2488.
34. Cramer WA, Sharma O, & Zakharov SD (2018) On mechanisms of colicin import: the outer membrane quandary. *Biochem J* 475(23):3903-3915.
35. Mohanty AK, Bishop CM, Bishop TC, Wimley WC, & Wiener MC (2003) Enzymatic E-colicins bind to their target receptor BtuB by presentation of a small binding epitope on a coiled-coil scaffold. *The Journal of biological chemistry* 278(42):40953-40958.
36. Taylor R, Burgner JW, Clifton J, & Cramer WA (1998) Purification and characterization of monomeric Escherichia coli vitamin B12 receptor with high affinity for colicin E3. *The Journal of biological chemistry* 273(47):31113-31118.
37. Spector J*, et al.* (2010) Mobility of BtuB and OmpF in the Escherichia coli outer membrane: implications for dynamic formation of a translocon complex. *Biophysical journal* 99(12):3880-3886.
38. Tikhonova EB & Zgurskaya HI (2004) AcrA, AcrB, and TolC of Escherichia coli Form a Stable Intermembrane Multidrug Efflux Complex. *The Journal of biological chemistry* 279(31):32116-32124.
39. Franklin MW*, et al.* (2018) Efflux Pumps Represent Possible Evolutionary Convergence onto the beta-Barrel Fold. *Structure* 26(9):1266-1274.e1262.
40. Kleanthous C (2010) Swimming against the tide: progress and challenges in our understanding of colicin translocation. *Nat Rev Microbiol* 8(12):843-848.
41. Tuson HH & Biteen JS (2015) Unveiling the inner workings of live bacteria using super-resolution microscopy. *Anal Chem* 87(1):42-63.

Supplemental Data

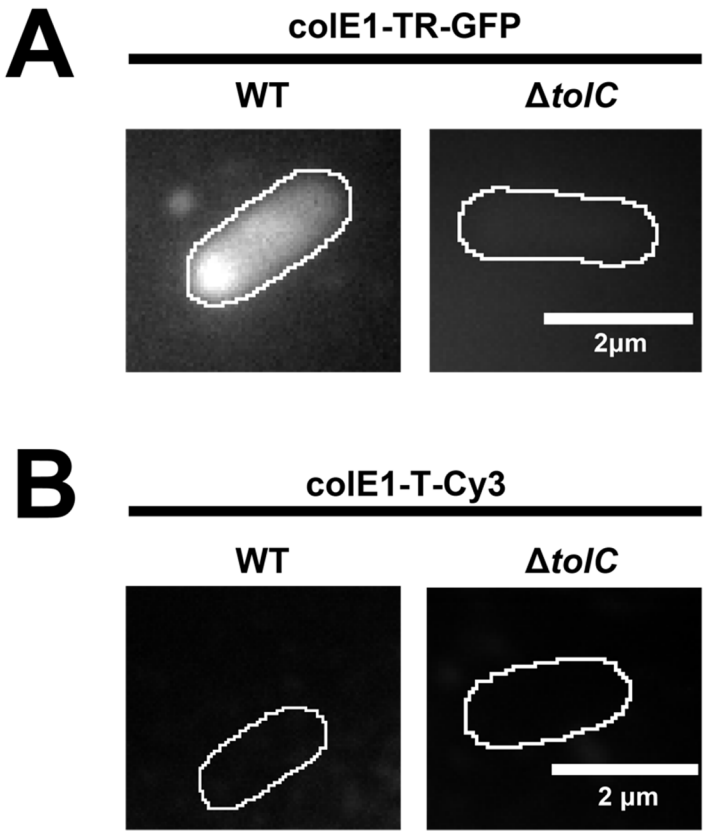

Figure S1: Single-molecule microscopy. Fluorescence images of colE1-TR-GFP (A) and Cy3-labeled colE1-T (B) overlaid on outlines of living *E. coli* cells from phase-contrast microscopy for WT and Δ*tolC*. Scale bar: 2 μm. ColE1-TR-GFP forms similar puncta as Cy3-labeled ColE1-TR. No binding of Cy3-labeled colE1-T to WT or Δ*tolC* cells was detected.

Movie S1 Caption:

616 Colicin E1 TR localizes on, and remains bound to, the extracellular surface of E. coli.
617 Fluorescence movie of Cy3-labeled colE1-TR on living WT E. coli overlaid on outline of
618 the E. coli cell from phase-contrast microscopy. Continuous imaging at 25 frames per
619 second. Scale bar: 2 μm.
620

621

Table S1

Minimum inhibitor concentrations of antimicrobials in the presence of colE1-TR

	Erythromycin (μg/mL)	Ciprofloxacin (ng/mL)	Kanamycin (μg/mL)	Benzalkonium Chloride (μg/mL)
WT	255.0 ±11.7	39.4 ±2.7	14.0 ±2.3	42.2 ±4.0
ΔtolC	2.5 ±0.1	4.0 ±0.3	NA	3.3 ±0.3
WT + 1 μM colE1-TR	298.7 ±13.6	53.5 ±7.2	15.7 ±3.3	48.49 ±7.5
WT + 10 μM colE1-TR	271.7 ±22.9	50.2 ±18.0	15.1 ±5.2	48.3 ±0.9
WT + 25 μM colE1-TR	162.6 ±5.8	42.3 ±7.3	5.4 ±1.2	38.6 ±5.5
WT + 50 μM colE1-TR	167.0 ±15.0	34.6 ±9.2	19.1 ±3.0	45.5 ±0.3
WT + 100 μM colE1-TR	111.8 ±27.6	25.0 ±4.7	6.8 ±2.2	20.7 ±2.8
fold change in MIC at 100 μM colE1-TR	2.2x	1.6x	2.0x	2.0x

± denote Standard Error of the Mean (SEM)

Supplementary Methods

Expression and Purification

Colicin E1 constructs

The gene for WT colE1-TR was synthesized as a double-stranded linear fragment (Integrated DNA Technologies) and cloned into pET303 using megaprimer restriction free cloning. Inverse PCR was used to delete the R domain and produce colicin E1-T. The gene for colicin E1-TR-GFP was produced by inserting GFP upstream of colE-TR, using Gibson assembly. Plasmids were transformed into *E. coli* BL21(DE3) cells and plated on LB + agar + 100 µg/mL carbenicillin. Single colonies were inoculated into 50 mL LB broth with 100 µg/mL carbenicillin and grown overnight at 37 °C with shaking at 250 r.p.m. Proteins were expressed by inoculating 1L of TB supplemented with 0.4% glycerol, 10 mM MgCl2 and 100 µg/mL carbenicillin with 20 mL of the overnight culture; the culture was grown at 37 °C to an OD_{600} of 2.0 and induced with 1 mM IPTG. Expression cultures were grown at 15 °C for 24 hours and harvested at 4,000g for 30 minutes at 4 °C. Cell pellets were resuspended in (3 mL/g of cell pellet) lysis buffer (TBS, 5 mM MgCl2, 10 mM imidazole, 1mM PMSF, 10 µg/mL DNase, 0.25 mg/mL lysozyme) and lysed via sonication (2 minutes, 2s on, 8s off, 40% amplitude, QSonica Q500 with 12.7 mm probe) in an ice bath. Lysates were centrifuged at 4,000g for 10 minutes to remove un-lysed cells and debris. The supernatant was centrifuged again at 20,000 r.p.m. in a Beckman Coulter J2-21 for 1 hour at 4 °C. Clarified lysates were applied to a 5 mL HisTrap FF column and purified using an ÄKTA FPLC system with a 20 column volume wash step with binding buffer (TBS, 25 mM imidazole) and eluted using a linear gradient from 0-50% elution buffer (TBS, 500 mM imidazole) in 10 column volumes. Proteins were concentrated in Amicon centrifugal filters with molecular weight cutoffs of 10K and 30K for colicin E1-T and for colicin E1-TR, respectively.

Concentrated proteins were loaded onto a HiLoad Superdex 16/60 200 pg gel filtration column and eluted into phosphate buffered saline (PBS) pH 7.4.

TolC

The gene for full-length TolC (a generous gift from R. Misra) was cloned into pTrcHis with a C-terminal 6x histidine tag. Plasmids were transformed into BL21(DE3)Omp8 and plated on LB + agar + 100 µg/mL carbenicillin. A single colony was picked and grown in LB-Lennox at 30 °C with shaking at 150 r.p.m. overnight. In the morning, 1L of LB-Lennox was inoculated with 20 mL of the overnight culture and grown at 30 °C with shaking at 150 r.p.m. until the culture reached an OD_{600} of 0.6, at which point protein expression was induced with 1mM IPTG for an additional 4 hours then harvested at 4,000g for 30 minutes at 4°C. Cell pellets were resuspended in 30 mL of Lysis buffer (TBS, 5 mM $MgCl_2$, 5 µg/mL DNase, 1mM PMSF) and lysed via sonication (2 minutes, 2s on, 8s off, 40% amplitude, QSonica Q500 with 12.7 mm probe) in an ice bath. Cell lysates were centrifuged at 4,000 g for 30 minutes at 4 °C to remove un-lysed cells and inclusion bodies. Total membrane fractions were harvested by centrifuging at 20,000 r.p.m. in a Beckman Coulter J2-21 for 1 hour at 4 °C. The resulting membrane pellet was resuspended in 20 mM Tris, 400 NaCl, 1% n-dodecyl-β-D-maltoside with mild stirring at 4 °C overnight to extract the protein. The solubilized membrane fraction was centrifuged at 20,000 r.p.m. in a Beckman Coulter J2-21 for 1 hour at 4 °C. The supernatant was filtered through 0.22 µm and applied to a 1 mL HisTrap FF column and purified using an ÄKTA FPLC system with a 20 column volume wash step with binding buffer (20 mM Tris, 400 NaCl, 0.05% n-dodecyl-β-D-maltoside, 25 mM imidazole) and eluted using a linear gradient from 0-100% elution buffer (20 mM Tris, 400 NaCl, 0.05% n-dodecyl-β-D-maltoside, 500 mM imidazole) in 10 column volumes. TolC containing fractions were pooled and concentrated to 2 mL and applied onto a HiLoad 16/60

677 Superdex 200 pg column and eluted with 1.5 column volumes in 20 mM Tris, 400 NaCl,
678 0.05% n-dodecyl-β-D-maltoside.
679
680 *Extracellular Protease Digestion*
681 Protein localization after exogenous protein addition to whole cells was
682 determined as previously described (1). BW25113 cells were grown to an OD_{600} of ~0.6.
683 Cells were harvested by centrifugation at 4,000g for 5 minutes and resuspended in 1x
684 PBS. Cells were incubated with 10 μM protein and incubated for 1 hour at 37 °C with
685 rocking. After incubation, cells were harvested by centrifugation and washed 2x with
686 PBS to remove any unbound protein. Cell pellets were resuspended in 5 mL of protease
687 buffer (50 mM Tris pH=8, 7.5 mM $CaCl_2$) and OD_{600} normalized. Cultures were split into
688 two samples for trypsin digestion: 1) intact cells 2) lysed cells. For the lysed cell sample,
689 0.25 mg/mL lysozyme was added, and the sample was incubated at room temperature
690 for 15 minutes. The cells were lysed by 5x freeze-thaw cycles by submerging in liquid
691 nitrogen followed by thawing. For each cell condition (lysed and intact) the sample was
692 further split into 6 aliquots. Aliquots were incubated with a final concentration of 0, 5, 20
693 μg/mL trypsin. The reaction was incubated for 30 minutes with intermittent gentle flicking
694 of the tubes. After 30 minutes 100 mM PMSF was added to stop the digestion reaction.
695 Samples were snap frozen in liquid nitrogen and stored at -20 °C until western blot
696 analysis.
697
698 *Single-Molecule Microscopy*
699 Cysteine mutants for microscopy were purified as described above with the
700 addition of 1 mM TCEP in all buffers to prevent covalent dimer formation. Because of the
701 use of the fluorophore, all subsequent steps were performed with limited exposure to
702 light and in amber tubes. Cyanine3 (Cy3) maleimide (Lumiprobe) was reconstituted in

DMSO. Fluorophore labeling was achieved by mixing a 20-fold molar excess of Cy3 maleimide to protein and incubating overnight at 4 °C. Free dye was removed by gel filtration on a Sephadex NAP-10 G-25 column. The sample was simultaneously buffer-exchanged into storage buffer (PBS pH 7.4, 1 mM DTT, 1 mM EDTA). The degree of labeling was determined spectrophotometrically from the concentrations of the dye and protein solutions using their respective extinction coefficients, ε, as described by their manufacturers or for the proteins as estimated by Expasy ProtParam (Cy3 ε_{548nm} = 162,000 L mol^{-1} cm^{-1}; colE1-T-E192C ε_{280nm} = 9,970 L mol^{-1} cm^{-1}; colE1-TR-E366C ε_{280nm} = 14,440 L mol^{-1} cm^{-1}). Labeling efficiencies were ~75% and ~85% for colE1-T-E192C and colE1-TR-E366C, respectively. Protein concentrations were adjusted according to the percentage of labeled protein.

Cultures of *E. coli* (BW25113 or Δ*tolC*) were grown in LB medium at 37 °C with shaking (180 r.p.m.) overnight, then transferred to MOPS minimal medium (Teknova) with 0.2% glycerol and 1.32 mM K_2HPO_4, and grown at 37 °C for 13 h. A sample was transferred to MOPS medium and grown to turbidity at 37 °C overnight. A 1-mL aliquot of culture was centrifuged for 2 min at 4850g to pellet the cells. The pellet was washed in 1 mL MOPS and centrifuged a second time. The supernatant was then removed, and the cell pellet was resuspended in 500 µL MOPS. A 1.0 µL droplet of concentrated cells was placed onto a glass slide. Then, a 1.0 µL droplet of 1 µg/mL colicin E1 protein construct stock was added to the cells. The droplet was covered by an agarose pad (1% agarose in MOPS media) and a second coverslip.

Samples were imaged at room temperature using wide-field epifluorescence microscopy with sensitivity to detect single dye molecules as described previously (2). Briefly, fluorescence was excited by a 561-nm laser (Coherent Sapphire 560-50) for Cy3 or a 488-nm laser (Coherent Sapphire 488-50) for GFP. The lasers were operated at low power densities (1 – 2 W/cm^2), and fluorescence was imaged with an Olympus IX71

729 inverted microscope with a 100x, 1.40-NA oil-immersion objective and appropriate
730 excitation, emission, and dichroic filters. A Photometrics Evolve electron multiplying
731 charge-coupled device (EMCCD) camera with > 90% quantum efficiency captured the
732 images at a rate of 20 frames per second. Each detector pixel corresponds to a 49 nm ×
733 49 nm area of the sample.
734
735 *Real-time Efflux*
736 Real-time efflux activity in the presence of colE1-TR was determined as
737 previously described with some modifications (3,4). A single colony of *E. coli* BW25113
738 was inoculated into 10 mL of LB and incubated overnight at 37 °C. The next day, 50 mL
739 of LB was inoculated with 1 mL of the overnight culture and grown to OD_{600} of ~0.8.
740 Cells were pelleted at 3,500g for 5 minutes. Cells were resuspended to OD_{600} 1.5 in cold
741 PBS with and without 10-100 μM colicin proteins and incubated for 15 minutes on ice. To
742 decouple proton motive force and turn off efflux, 100μM carbonyl cyanide m-
743 chlorophenyl hydrazone (CCCP) was added. After an additional 15 minutes the efflux
744 dye NNN was added to the cells to 10 μM. The cells were incubated at 25 °C with
745 shaking at 140 r.p.m. for 2 hours. Cells were harvested at 3,500g for 5 minutes and
746 washed once in 20 mM potassium phosphate buffer pH 7 with 1mM $MgCl_2$. Optical
747 densities were adjusted to OD_{600} 1.0 and placed on ice. Then, 2 mL of the cell
748 suspension was loaded into a quartz cuvette (Agilent Technologies). Fluorescence was
749 measured with an Agilent Cary Eclipse fluorescence spectrophotometer with slit widths
750 at 5 and 10 nm for excitation wavelength of 370 nm and emission wavelength of 415 nm.
751 Fluorescence measurements were taken every 1 second. After 100 seconds, 50 mM
752 glucose was added to re-energize the cells and initiate efflux, and fluorescence data
753 were collected for an additional 600 seconds.
754

Modeling BtuB and TolC on a grid

To select the configurations where every pair of BtuB and TolC proteins interact, we transformed each of the 24-choose-12 grid configurations (equation 1) into a bipartite graph representation where two vertices are connected by an edge if they are neighbors in the grid. Neighbors are defined as if a BtuB is one of the 8 immediate neighbors of a TolC. We applied the Hopcroft-Karp algorithm (5) for finding a maximum cardinality matching on the graph. If a matching was found this was counted as one successful configuration.

The number of successful configurations was 788,736. Removing the three symmetries of the rectangle (vertical and horizontal plane flips and 180-degree rotation), the number is 788,736/3 = 262,912. In neither the 24 choose 12 set nor the neighboring set if a configuration is the same as its mirror image (vertical or horizontal), these are not counted as separate instances.

equation 1.

$$\frac{24!}{12!\,(24-12)!} = 2{,}704{,}156$$

Supplementary References

1. Besingi RN & Clark PL (2015) Extracellular protease digestion to evaluate membrane protein cell surface localization. *Nature protocols* 10(12):2074-2080.
2. Tuson HH & Biteen JS (2015) Unveiling the inner workings of live bacteria using super-resolution microscopy. *Anal Chem* 87(1):42-63.
3. Bohnert JA, Karamian B, & Nikaido H (2010) Optimized Nile Red efflux assay of AcrAB-TolC multidrug efflux system shows competition between substrates. *Antimicrob Agents Chemother* 54(9):3770-3775.

4. Bohnert JA, Schuster S, Szymaniak-Vits M, & Kern WV (2011) Determination of real-time efflux phenotypes in Escherichia coli AcrB binding pocket phenylalanine mutants using a 1,2'-dinaphthylamine efflux assay. *PloS one* 6(6):e21196.
5. Hopcroft JE & Karp RM (1973) An $n^{5/2}$ Algorithm for Maximum Matchings in Bipartite Graphs. *SIAM Journal on Computing* 2(4):225-231.